

## Research Article

# Effect of Ultrasonic Flexural Vibration on Solidification Structure and Mechanical Properties of Large-Size 35CrMoV Cast Ingot

Chen Shi <sup>1,2</sup>, Fan Li,<sup>1</sup> Yongjun Wu,<sup>1</sup> and Daheng Mao<sup>1</sup>

<sup>1</sup>College of Mechanical and Electrical Engineering, Central South University, Changsha 410083, China

<sup>2</sup>National Key Laboratory of High Performance Complex Manufacturing, Central South University, Changsha 410083, China

Correspondence should be addressed to Chen Shi; [shichen@csu.edu.cn](mailto:shichen@csu.edu.cn)

Received 22 December 2018; Accepted 20 February 2019; Published 26 June 2019

Academic Editor: Hongchao Kou

Copyright © 2019 Chen Shi et al. This is an open access article distributed under the Creative Commons Attribution License, which permits unrestricted use, distribution, and reproduction in any medium, provided the original work is properly cited.

In order to improve the performances of large-size 35CrMoV cast ingot, ultrasonic flexural vibration was guided into 35CrMoV steel melt through L-shaped ultrasonic waveguide rod during the solidification, and the effects of ultrasonic flexural vibration on macrostructure, microstructure, and mechanical properties of large-size 35CrMoV cast ingot were investigated. It is found that the columnar crystal zone has disappeared and the ingot is composed of the equiaxed crystals present in the ultrasonic ingot. The size of grains treated by ultrasonic are significantly smaller than conventional ingot. The distribution of ferrite in matrix structure is also more uniform than conventional ingot. The tensile strength is increased by 3.14%~17.12%, and the elongation is increased by 39.13%~287.50% compared with the conventional ingot at different positions.

## 1. Introduction

The large-size cast ingots produced by traditional mould casting process have many problems such as developed columnar crystals, serious composition segregation, coarse shrinkage cavities, and so on. With the development of ultrasonic technology, researchers have found that ultrasonic can generate a series of physical phenomenon such as cavitation, acoustic flow, and resonance when it propagates in melt. These phenomena could effectively refine the microstructure and improve the mechanical properties, but the studies and applications of ultrasonic casting are mainly concentrated in the field of nonferrous metals [1–11], and the study on ultrasonic casting in the steel field is rare and still at the laboratory research stage.

Liu et al. [12] treated 1Cr18Ni9Ti steel ingots whose size was 120 mm × 60 mm × 60 mm, and it was found that the dendrites of long strip were broken and transformed into equiaxed crystals. Liu et al. [13] carried out the tensile test of high carbon steel ingots with the size of 14 mm × 60 mm × 60 mm at ambient temperature, and they found that the tensile strength of the ingot was increased by 30% and the elongation was increased by 1.5 times through

ultrasonic treatment. Kang et al. [14] introduced ultrasonic into the 304 stainless steel melt with height of 36 mm and found that the effect of grain refinement became more obvious with the increase of ultrasonic power. Kong et al. [15] treated the solidification process of low carbon steel ingot whose size was F55 mm × 120 mm with ultrasonic, and the result demonstrated that the grain size decreased from 550 μm to 140 μm and Widmanstätten disappeared from the matrix structure. Nowacki [16] implemented an experiment exploring the effect of ultrasonic treatment on high carbon steel ingot with a weight of 130 kg; the result showed that the V-shaped segregation was alleviated in the central region after ultrasonic treatment.

In summary, researchers found that the effect of ultrasonic casting in small-size steel ingots is very obvious. However, there is no study on the ultrasonic casting of large-size steel ingots because there are still many difficulties in the application of ultrasonic casting in large-size steel ingots. The most important factor is that the titanium alloy sonotrode which is widely used in nonferrous metal ultrasonic casting is easy to be dissolved in molten steel. Li et al. [17] have studied the material of the sonotrode and found that few materials could resist the corrosion of steel melt. This

factor makes it extremely difficult to introduce ultrasonic wave into steel melt for a long time. Moreover, ultrasonic wave is guided into melt through straight ultrasonic waveguide rod traditionally, whose disadvantage is that the upward thermal radiation of the molten steel can decrease the effective life of the ultrasonic transducer.

In order to solve these problems, we successfully developed a kind of nanoceramic material that can effectively slow down the dissolution of sonotrode in steel melt, and we designed the T-shaped ultrasonic waveguide rod, which could successfully avoid the damage of the upward thermal radiation to the ultrasonic transducer [18, 19]. In order to improve the performances of large-size cast ingot, we revised the sizes of ultrasonic waveguide rod and changed T-shaped rod into L-shaped rod that can produce flexural vibration and strengthen vibration's radial propagation in large-size steel melt, while the traditional straight ultrasonic waveguide rod produces longitudinal vibration and makes it propagate along axis direction. In this paper, ultrasonic flexural vibration was guided into 35CrMoV steel melt through L-shaped ultrasonic waveguide rod, and the influences of ultrasonic flexural vibration on macrostructure, microstructure, and mechanical properties of large-size 35CrMoV cast ingot were investigated.

## 2. Materials and Methods

**2.1. Materials.** The material studied in this paper is 35CrMoV steel, whose proportion of the main components is shown in Table 1. The diameter of ingot is 440 mm at the riser and 380 mm at the tail, the height is 800 mm, and the weight is nearly 1000 kg, as shown in Figure 1.

**2.2. Ultrasonic Equipment.** The experimental device for ultrasonic casting includes two acoustic systems, as shown in Figure 2. Each acoustic system is made up of one ultrasonic generator (the range of generator power is 0 W–1200 W and adjustable, the frequency of generator is  $25 \pm 0.5$  kHz, and the output amplitude is  $10 \mu\text{m}$ ), one ultrasonic transducer, one L-shaped ultrasonic waveguide rod that is composed of two-stage ultrasonic amplitude amplifier pole, and a nanoceramic sonotrode. Firstly, the ultrasonic generator converts 220 V, 50 Hz alternating current into a 25.3 kHz high-frequency oscillation signal. Secondly, the piezoelectric transducer transforms the electrical signal into the 25.3 kHz ultrasonic longitudinal vibration. Then, the amplitude of ultrasonic vibration is amplified and the vibrational mode is changed into flexural vibration through L-shaped ultrasonic waveguide rod. Finally, ultrasonic flexural vibration is guided into steel melt through the nanoceramic sonotrode that is submerged in the melt.

**2.3. Experimental Process of Ultrasonic Casting.** The schematic diagram of ultrasonic casting is shown in Figure 3. Sand mould was used in this experiment. The melt of 35CrMoV was heated to  $1630^\circ\text{C}$  in medium frequency induction furnace and then was poured into two sand moulds from the bottom of the cavity through runner. The ultrasonic sonotrode was inserted into the steel melt in one sand mould

TABLE 1: Composition in mass % of 35CrMoV steel employed.

Chemical composition	C	Si	Mn	Cr	Mo	Ni	V	Fe
Mass fraction	0.34	0.25	0.60	1.20	0.27	0.02	0.17	Bal.



FIGURE 1: 35CrMoV steel ingots.

with the insertion depth of 80 mm. The working parameters of ultrasonic equipment are shown in Table 2. The sonotrode was taken out from the melt when the ultrasonic treatment time reached the predetermined time. Then, the ingots were naturally cooled in the sand mould. Another ingot was cast by the conventional treatment.

**2.4. Experimental Detection.** Samples for analysis were cut from the ingots with and without ultrasonic treatment at the same positions; Figure 4 shows the sampling positions.

The macrostructure samples were polished on grinding machine until the surface roughness was less than  $Ra1.6$ . The samples were etched by 25% nitric acid solution. Then, the macrostructure of ingots were observed using low-magnification microscope.

The microstructure samples were ground and polished and then etched by the 1:1 hydrochloric acid solution which was heated to  $70^\circ\text{C}$ . The grain sizes of samples were observed by an optical microscope (OM, OLYMPUS DSX500, Tokyo, Japan).

The as-cast ferrite structure samples were corroded with 4% nitric acid alcohol for dozen of seconds. The as-cast ferrite structures of the samples were observed by the optical microscope.

A group of tensile samples were taken at  $0R$ ,  $1/2R$ , and  $R$  of the ingots. Each group had three parallel samples. The size of the tensile sample is shown in Figure 5. The tensile tests were implemented on MTS 322 universal material testing machine at ambient temperature. The loading rate of the

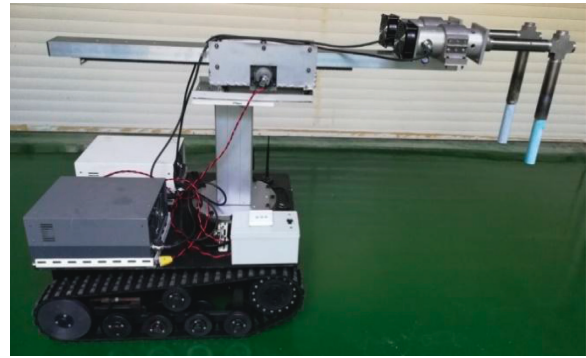
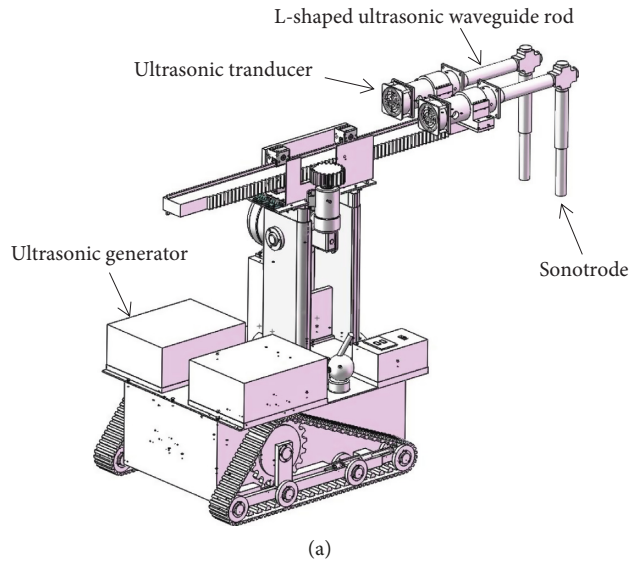


FIGURE 2: The ultrasonic equipment.

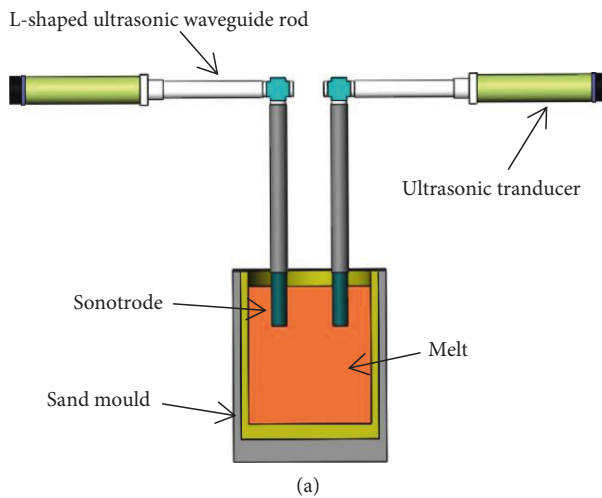


FIGURE 3: Schematic diagram and photo of ultrasonic casting.

TABLE 2: The key parameters of ultrasonic device.

Input power (W)	Frequency (kHz)	Amplitude (um)	Operating time (min)
2000	25.3	10	30

tensile process was 0.5 mm/min. The yield strength, tensile strength, elongation, and section shrinkage of the samples were measured.

### 3. Results and Discussion

**3.1. Effect of Ultrasonic Flexural Vibration on Macrostructure of 35CrMoV Ingot.** Figure 6 shows the macrostructure of the ingot surfaces. Figure 6(a) is the surface morphology of the conventional ingot, and it shows that the columnar crystal zone accounting for 20.8% of the cross section grows

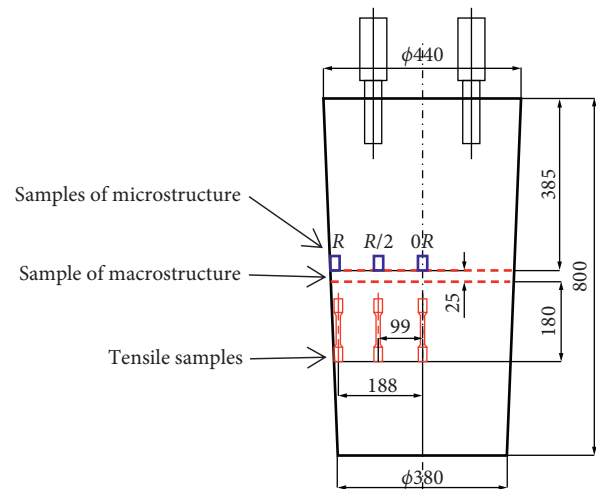


FIGURE 4: The sampling positions.

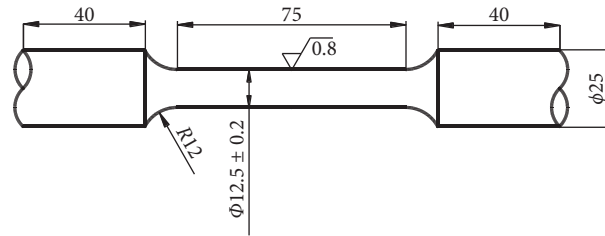


FIGURE 5: The size of tensile sample.

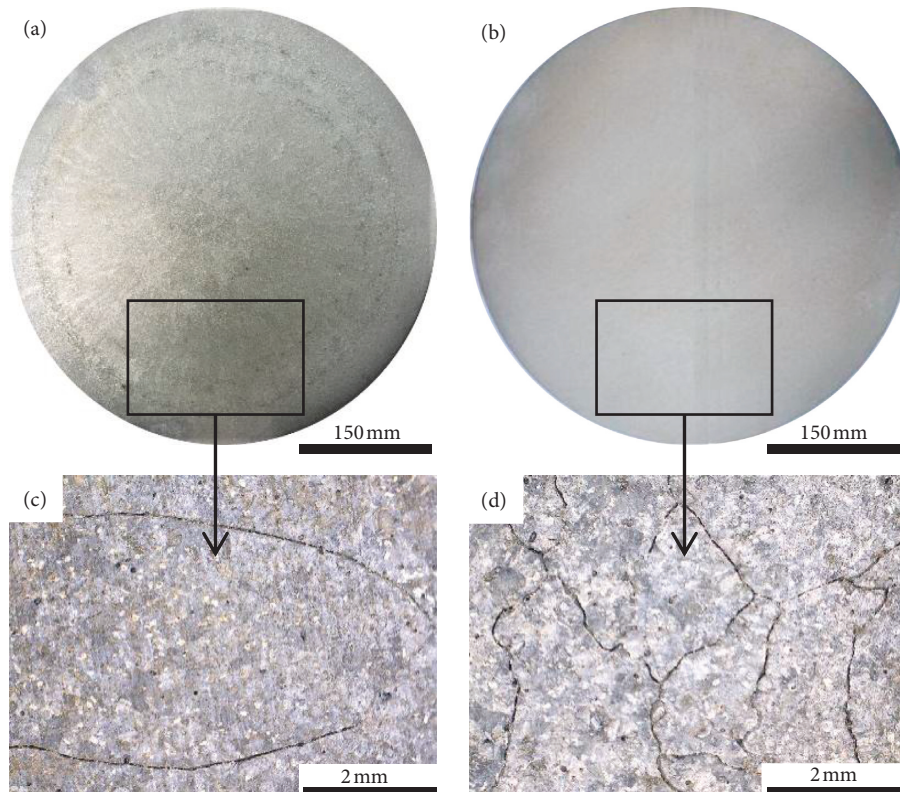


FIGURE 6: Macrostructures of ingots: (a) conventional ingot; (b) ultrasonic ingot; (c) edge morphology of the conventional ingot; (d) edge morphology of the ultrasonic ingot.

perpendicularly to the center from the die wall, and the coarse equiaxed crystal zone in the middle of the sample accounts for 79.2%. The edge morphology of conventional ingot was observed through a low-magnification microscope (40x), as shown in Figure 6(c), and it can be seen that the columnar crystal whose length is up to 20 mm is obvious. Figure 6(b) is the surface morphology of the ultrasonic ingot, where there is no obvious columnar crystal zone and the equiaxed crystals are irregular in shape distributing from the edge to the center. Figure 6(d) is the edge morphology of ultrasonic ingot, which indicates that the grains grow freely.

When ultrasonic flexural vibration was guided into 35CrMoV steel melt through the L-shaped ultrasonic waveguide rod, a large pressure gradient is formed at the ultrasonic wave surface and leads to instantaneous changes of positive pressure and negative pressure resulting in a local high temperature and high pressure, which scours the solidification front along the radial direction and destroys the columnar dendrites that are nucleating and growing at the

solid-liquid interface in the process of crystallization. The broken crystalline phases distribute uniformly to the various parts of the ingot along with the turbulent liquid steel and become a new sprouting crystal that forms a large number of equiaxed crystal nuclei. Therefore, the columnar crystal zone decreases or even disappears and equiaxed crystal region extends to the whole region of ultrasonic ingot.

*3.2. Effect of Ultrasonic Flexural Vibration on As-Cast Grain of 35CrMoV Ingot.* The grain size of cast ingot has great influence on the mechanical properties of ingot. The finer the ingot grains are, the higher the strength of the casting is and the stronger the ability to resist plastic deformation is. Figures 7(a)–7(c) show the as-cast grains of conventional ingot. The columnar crystals grow perpendicularly from the edge to the center, as shown in Figure 7(a), and the length of single columnar crystal is up to 21 mm. The samples at 1/2R and 0R are all equiaxed crystals whose size is not

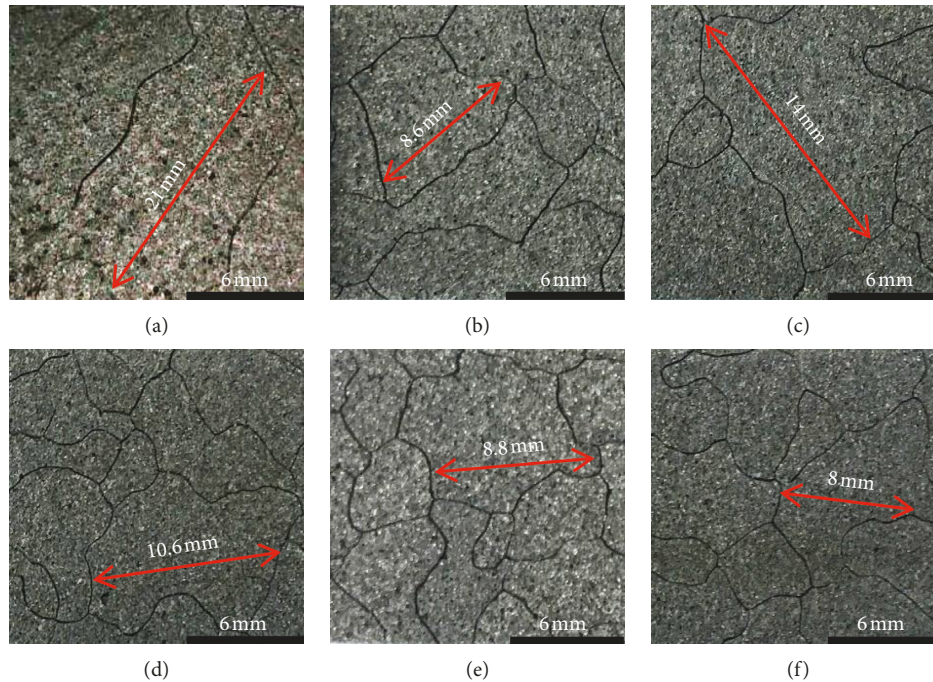


FIGURE 7: Microstructure of the ingots: (a) the conventional ingot at position  $R$ ; (b) the conventional ingot at position  $1/2R$ ; (c) the conventional ingot at position  $0R$ ; (d) the ultrasonic ingot at position  $R$ ; (e) the ultrasonic ingot at position  $1/2R$ ; (f) the ultrasonic ingot at position  $0R$ .

homogeneous. The grain has the tendency to grow up from position  $1/2R$  to the center. The diameter of the single equiaxed crystal reaches 14 mm in the center. Figures 7(d)–7(f) show the as-cast grains of ultrasonic ingot, and it can be seen that the homogeneous equiaxed crystals distribute from the edge to the center and there is no columnar crystal zone in ultrasonic ingot.

Comparing Figures 7(a)–7(f), it is found that ultrasonic flexural vibration could effectively inhibit the growth of crystals and refine the as-cast grains and then make the sizes of as-cast grains more homogeneous.

Atoms in liquid metals are in constant heat motion which leads to the short range ordered atomic clusters that appear and disappear in an instant. This phenomenon increases the fluctuations that are the seeds of the nucleus in the liquid metal. The ultrasonic vibration in the melt accelerates the thermal motion of the atom, which increases the frequent occurrence and disappearance of the atomic group. This action accelerates the fluctuation of the phase in the liquid metal, which increases the number of crystal embryos and the nucleation rate. Moreover, the disturbance produced by ultrasonic flexural vibration has a strong stirring effect in the melt and makes the growing grains break in the melt, which not only increases the number of nuclei but also decreases the velocity of grain growth. Therefore, the application of ultrasonic flexural vibration in the solidification process is beneficial to obtain fine and homogeneous solidification microstructure.

**3.3. Effect of Ultrasonic Flexural Vibration on As-Cast Ferrite Structure of 35CrMoV Ingot.** Ferrite and pearlite are main components of as-cast structure of the 35CrMoV steel which

belongs to the hypoeutectoid steel. The white bulk is ferrite and the gray mass is pearlite, as shown in Figure 8. It is found that the number of bulk ferrite precipitated in conventional ingot is less than that in ultrasonic ingot. However, the size of massive ferrite in ultrasonic ingot is only  $1/2$ – $1/3$  of the conventional ingot. Therefore, ultrasonic flexural vibration makes the distribution of matrix more uniform.

**3.4. Effect of Ultrasonic Flexural Vibration on Mechanical Properties of 35CrMoV Ingot.** Figure 9 shows the comparison of mechanical properties between ultrasonic ingot and conventional ingot. Figure 9(a) shows the yield strength at three different positions. The yield strength of ultrasonic ingot increases about 11.18%–14.72% compared with conventional ingot. The yield strength at  $1/2R$  increases about 14.72%. The maximum yield strength of conventional ingot is 397.56 MPa, and the maximum yield strength of ultrasonic ingot is 442 MPa. Two kinds of ingots have the highest yield strength at  $0R$ . Figure 9(b) shows the tensile strength at three different positions. The tensile strength of ultrasonic ingot increases about 3.14%–17.12% compared with conventional ingot. The tensile strength at  $1/2R$  increased about 17.12% reaching to 622.1 MPa. The improvement of tensile strength at  $R$  is not obvious. Figures 9(c) and 9(d) are, respectively, the cross section shrinkage and elongation of conventional ingot and ultrasonic ingot at three different positions. The cross section shrinkage and elongation of ultrasonic ingot are higher than conventional ingot, and the elongation is increased by 39.13%–287.50% compared with the conventional ingot at different positions.

Figure 10 shows the fracture morphology of the tensile samples at ambient temperature. All these samples have no

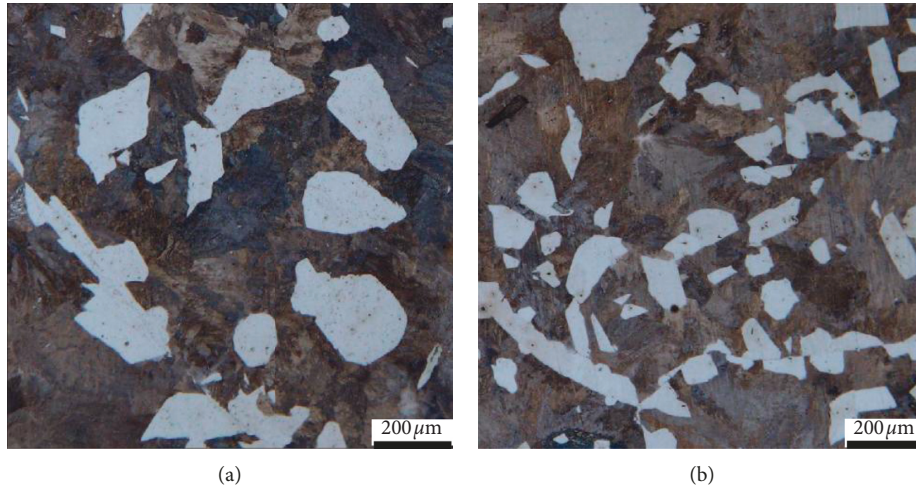


FIGURE 8: As-cast structures of the conventional ingot (a) and the ultrasonic ingot (b).

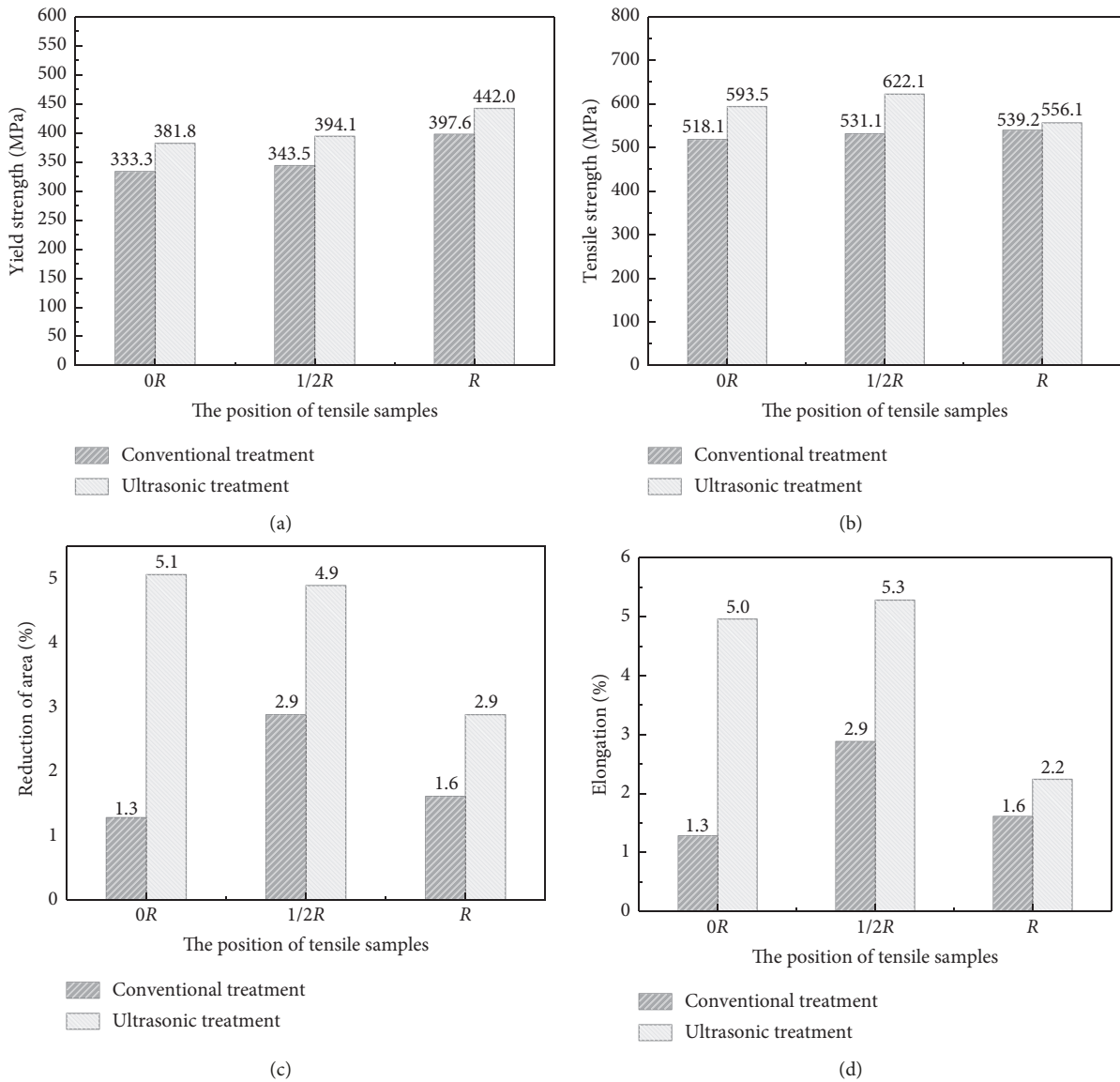


FIGURE 9: The mechanical properties of 35CrMoV ingots.

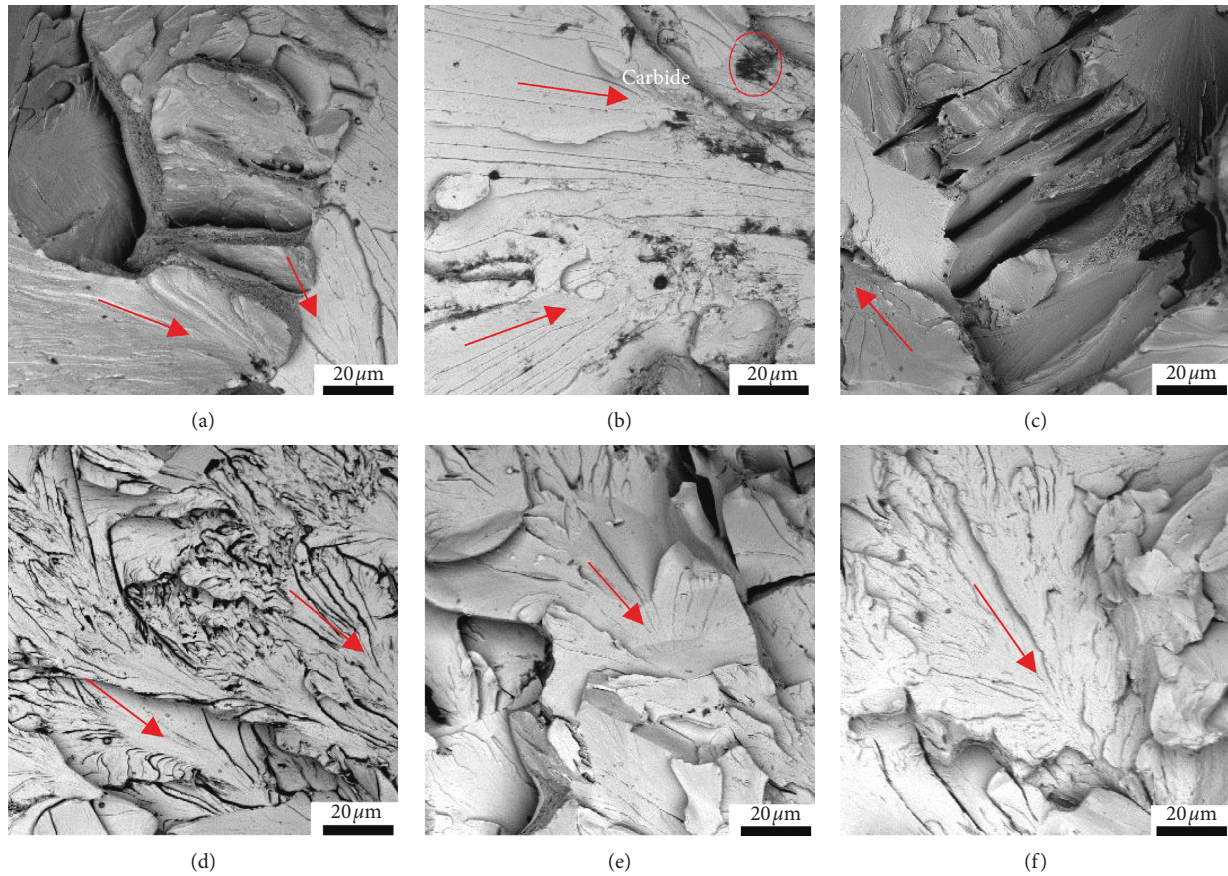


FIGURE 10: The fracture morphology of tensile specimens: (a) the conventional ingots at position  $R$ ; (b) the conventional ingots at position  $1/2R$ ; (c) the conventional ingots at position  $0R$ ; (d) the ultrasonic ingots at position  $R$ ; (e) the ultrasonic ingots at position  $1/2R$ ; (f) the ultrasonic ingots at position  $0R$ .

obvious macroscopic plastic deformation on the fracture surface. They belong to brittle fracture. Some typical fracture morphology was observed by the scanning electron microscope. The tensile fracture of the conventional ingot belongs to the cleavage fracture. The transgranular fracture is the main way of breaking. The crack propagates through the grain, and the red arrow is the direction of the crack growth. The fracture surface is a typical fluvial pattern. Carbides existing on the fracture surface at  $1/2R$  reduce the adhesion in the matrix and easily produce the crack source. The fracture surface of ultrasonic ingot is also the cleavage fracture. The transgranular fracture is also the main way of breaking. The fracture morphology is a typical fluvial pattern at  $0R$  and  $1/2R$ . Crack spreads across multiple cleavage planes forming the cleavage steps at  $1/2R$ . Fracture morphology belongs to the sector pattern at  $R$ .

The tensile properties of the ingots are closely related to the grain size, the microstructure, and internal defects. During the tensile process, the fine grains of ultrasonic ingot make deformation take place within more grains, which reduces stress concentration and make deformation uniformity. Moreover, fine grains have more grain boundaries, which makes the crack propagate and develop more difficulty. Moreover, the aggregated carbides existing in cast ingot were broken and dispersed uniformly in the matrix by

ultrasonic flexural vibration, which enhances the matrix structure. Therefore, the mechanical properties of ingot are improved by ultrasonic flexural vibration.

#### 4. Conclusions

In this paper, researchers who introduced ultrasonic flexural vibration into the solidification of the 35CrMoV ingots studied the effect of ultrasonic flexural vibration on the macrostructure, microstructure, and mechanical properties. Based on the experiments, the following conclusions could be drawn:

- (1) Ultrasonic flexural vibration could effectively inhibit the growth of columnar crystals, which makes columnar crystal zone decrease and the equiaxed crystal zone increase. At the same time, the coarse grains of ingot are refined by ultrasonic flexural vibration.
- (2) Ultrasonic flexural vibration makes the distribution of ferrite in the matrix more uniform, and the matrix structure is optimized.
- (3) Ultrasonic flexural vibration improves the mechanical properties of large-size 35CrMoV cast ingot. The yield strength is increased by 11.18%~

14.72%, the tensile strength is increased by 3.14%~17.12%, and the elongation is increased by 39.13%~287.50%.

### Data Availability

The data used in this paper are all from experiments. The pictures used to support the results of experiments are included in this paper. Finally, the data of histogram used to support the findings of this paper are available from the corresponding author upon request.

### Conflicts of Interest

The authors declare no conflicts of interest.

### Authors' Contributions

Chen Shi and Daheng Mao conceived and designed the experiments; Fan Li carried out the experiments; Fan Li and Yongjun Wu analyzed the data; Daheng Mao contributed reagents, materials, and analysis tools; and Fan Li wrote the paper.

### Acknowledgments

This research was supported by the National Basic Research Program of China (2014CB046702).

### References

- [1] J.-L. Laborde, A. Hita, J.-P. Caltagirone, and A. Gerard, "Fluid dynamics phenomena induced by power ultrasounds," *Ultrasonics*, vol. 38, no. 1-8, pp. 297-300, 2000.
- [2] S. Wang, L. Wu, L. Zheng et al., "Effects of ultrasonic vibration on solidification structure of Zn-55Al-1.6Si alloy," *Special Casting & Nonferrous Alloys*, vol. 31, no. 3, pp. 285-287, 2011.
- [3] Y. U. Kun, W. X. Li, and R. C. Wang, "Effects of heat treatment on microstructures and mechanical properties of ZK60 magnesium alloy," *Chinese Journal of Nonferrous Metals*, vol. 34, no. 1, pp. 46-49, 2007.
- [4] D. Gao, Z. Li, Q. Han, and Q. Zhai, "Effect of ultrasonic power on microstructure and mechanical properties of AZ91 alloy," *Materials Science and Engineering: A*, vol. 502, no. 1-2, pp. 2-5, 2009.
- [5] C. Shi, K. Shen, D. Mao, Y. Zhou, and F. Li, "Effects of ultrasonic treatment on microstructure and mechanical properties of 6016 aluminium alloy," *Materials Science and Technology*, vol. 34, no. 12, pp. 1511-1518, 2018.
- [6] C. Shi and K. Shen, "Twin-roll casting 8011 aluminium alloy strips under ultrasonic energy field," *International Journal of Lightweight Materials and Manufacture*, vol. 1, no. 2, pp. 108-114, 2018.
- [7] P. Yue, D. H. Mao, L. I. Jian-Ping et al., "Effect of electromagnetic-ultrasonic energy-field on structure and properties of roll-casting 3003 aluminum alloy strips," *Chinese Journal of Nonferrous Metals*, vol. 24, no. 3, pp. 615-623, 2014.
- [8] J. P. Li, P. Yue, and C. Shi, "Effect of ultrasonic/electromagnetic energy-field on structure and properties of cast-rolled 3003 aluminum alloy strips," *Advanced Materials Research*, vol. 881-883, pp. 1378-1384, 2014.
- [9] X. Jian, H. Xu, T. T. Meek, and Q. Han, "Effect of power ultrasound on solidification of aluminum A356 alloy," *Materials Letters*, vol. 59, no. 2-3, pp. 190-193, 2005.
- [10] H. Liu, X. Qiao, Z. Chen, R. Jiang, and X. Li, "Effect of ultrasonic vibration during casting on microstructures and properties of 7050 aluminum alloy," *Journal of Materials Science*, vol. 46, no. 11, pp. 3923-3927, 2011.
- [11] X. U. Ting, L. H. Zhang, L. I. Rui-Qing et al., "Numerical simulation and experimental study of multi-field coupling for semi-continuous casting of large-scale aluminum ingots with ultrasonic treatment," *Chinese Journal of Engineering*, vol. 38, no. 9, pp. 1270-1277, 2016, in Chinese.
- [12] Q. Liu, Y. Zhang, Y. Song et al., "Influence of ultrasonic vibration on mechanical properties and microstructure of 1Cr18Ni9Ti stainless steel," *Materials & Design*, vol. 28, no. 6, pp. 1949-1952, 2007.
- [13] Q. Liu, Q. Zhai, F. Qi, and Y. Zhang, "Effects of power ultrasonic treatment on microstructure and mechanical properties of T10 steel," *Materials Letters*, vol. 61, no. 11-12, pp. 2422-2425, 2007.
- [14] J. Kang, X. Zhang, Y. Hu, J. Ma, Y. Hu, and T. Huang, "Ultrasonic treatment of the 304 stainless steel melt," *ISIJ International*, vol. 54, no. 2, pp. 281-287, 2014.
- [15] W. Kong, D. Q. Cang, and J. H. Song, "Effects of ultrasonic treatment during the solidification process on the structure formation of low carbon steel," *Materials Transactions*, vol. 52, no. 9, pp. 1844-1847, 2011.
- [16] K. Nowacki, "Influence of ultrasonic treatment on the structure of high-carbon steel," *Metallurgija*, vol. 50, no. 3, pp. 213-216, 2011.
- [17] J. Li, W. Chen, and B. He, "Study of probe material for ultrasonic treatment of molten steel," *Journal of University of Science and Technology Beijing*, vol. 29, no. 12, pp. 1246-1249, 2007, in Chinese.
- [18] G. Liang, C. Shi, Y. Zhou et al., "Effect of ultrasonic treatment on the solidification microstructure of die-cast 35CrMo steel," *Metals*, vol. 6, no. 11, p. 260, 2016.
- [19] G. Liang, C. Shi, Y.-j. Zhou, and D.-h. Mao, "Numerical simulation and experimental study of an ultrasonic waveguide for ultrasonic casting of 35CrMo steel," *Journal of Iron and Steel Research International*, vol. 23, no. 8, pp. 772-777, 2016.



**Hindawi**  
Submit your manuscripts at  
[www.hindawi.com](http://www.hindawi.com)

